AIAA JOURNAL
Vol. 42, No. 11, November 2004

Finite Element Multiple-Mode Approach to Nonlinear Free Vibrations of Shallow Shells

Adam Przekop,* M. Salim Azzouz,† Xinyun Guo,† and Chuh Mei‡
Old Dominion University, Norfolk, Virginia 23529
and
Lahcen Azrar§
Universite Abdelmalek Essaadi, Tanger, Morocco

Two finite element (FE) modal formulations for large-amplitude free vibration of isotropic and arbitrary laminated composite shallow shells are presented. The system equation of motion is formulated first in the physical structural node degrees of freedom (DOF). Then the system is transformed into two distinctly different sets of general Duffing-type modal equations based on 1) modal amplitudes of coupled linear bending and in-plane modes, where in-plane inertia is included in the formulation, and 2) modal amplitudes of linear bending modes only, where the in-plane inertia is neglected. Multiple modes and the first-order transverse shear deformation are considered in the formulations. A shallow-shell finite element is developed as an extension from the triangular Mindlin (MIN3) plate element with the improved shear correction factor by Tessler. Time numerical integration is employed to determine the nonlinear periodic frequency characteristics. The inaccuracy in characterizing a shallow-shell response with coupled linear bending and in-plane modes is demonstrated and discussed by comparing with the FE solution in structural node DOF. Study cases include isotropic and composite panels of different shallow-shell geometries.

Nomenclature

$[A]$ = in-plane material stiffness matrix
$[A_s]$ = shear material stiffness matrix
a = panel length
$[B]$ = coupled in-plane bending material stiffness matrix
b = panel width
$[D]$ = bending material stiffness matrix
h = panel thickness
$[\underline{K_L}]$ = linear stiffness matrix
$[\bar{K}_L]$ = modal linear stiffness matrix
$[K_q]$ = modal first-order nonlinear stiffness matrix
$[K_{qq}]$ = modal second-order nonlinear stiffness matrix
$[K_1]$ = first-order nonlinear stiffness matrix
$[K_2]$ = second-order nonlinear stiffness matrix
$[M]$ = mass matrix
$[\bar{M}]$ = modal mass matrix
q = generalized (modal) coordinate
R = shell radius
T = period
t = time
$\{U\}$ = in-plane displacement along x axis
$\{V\}$ = in-plane displacement along y axis
$\{W\}$ = transverse displacement
$\{\gamma_s\}$ = shear strain
$\{\varepsilon^0\}$ = in-plane strain
$\{\kappa\}$ = bending curvature
ν = Poisson ratio
$\{\phi\}$ = eigenvector
$\{\psi\}$ = rotation of normal to the midsurface
ω = frequency

Subscripts and Superscripts

b = bending
L = linear
m = membrane
max = maximum
min = minimum
N_b = referring to $[B]\{\kappa\}$
N_m = referring to $[A]\{\varepsilon_m^0\}$
N_R = referring to $[A]\{\varepsilon_R^0\}$
NL = nonlinear
R = radius
r = mode number
s = shear
t = transverse
x = x axis
y = y axis

Received 14 January 2003; presented as Paper 2004-1615 at the 45th Structures, Structural Dynamics, and Materials Conference, Palm Springs, CA, 19–22 April 2004; revision received 3 June 2004; accepted for publication 11 June 2004.

*Research Assistant, Department of Aerospace Engineering; currently Staff Scientist, National Institute of Aerospace, Hampton, VA 23666. Member AIAA.
†Research Assistant, Department of Aerospace Engineering. Student Member AIAA.
‡Professor, Department of Aerospace Engineering. Associate Fellow AIAA.
§Professor, Department of Mathematics, Faculty of Sciences and Techniques, B.P. 416.

Introduction

SHALLOW shells are common structural components in many fields of engineering. Various theories of shells were described and outlined in many monographs, for example, Refs. 1–3. A review of vibration of shallow shells covering the advances since the 1970s was given by Liew et al.[4] Based on an exhaustive literature search, the classical analyses of large-amplitude free vibration of shallow shells[5–12] have all neglected the in-plane inertia terms as a result of mathematical difficulties. Also difficulties in obtaining the initial conditions[13] for the steady periodic response resulted in the prevailing number of investigations using a single mode approximation.[5–7,9–11,14,15] Apart from the approach where a single-mode solution is obtained under the assumption of neglecting in-plane inertia, there are very few attempts departing from this pattern. Fu and Chia[8] and Abe et al.[12] accounted for multimode solution while in-plane inertia was dropped. On the other hand, Singh[16] and Sansour et al.[17] using energy methods included the membrane effects, but their energy estimations were based on

single-mode deformation. Moreover, classical solutions were usually obtained for simple geometry of rectangular planform, isotropic or orthotropic material, and fully simply supported or fully clamped boundary condition.

The much more versatile finite element (FE) methods, on the other hand, have dealt with this coupled linear bending and in-plane modes for flat unsymmetrically laminated composite plates (as a result of laminate stiffness $[B] \neq 0$). The general Duffing equations in terms of modal amplitudes of coupled linear bending in-plane modes were formulated by Shi et al.[18] for nonlinear free vibration of unsymmetric composite plates, whereas Abdel-Motaglay et al.[19] studied panel flutter with in-plane inertia neglected and the Duffing equations were expressed in terms of linear bending modal amplitudes. Przekop et al.[20] developed FE modal formulation for shallow-shell problems and addressed both in-plane inertia and multimode solution. Their approach, however, utilized the coupled linear bending and in-plane modes (caused by curvature and/or $[B] \neq 0$) and resulted in an overstiff response.

By neglecting the in-plane inertia terms and using classic analytical method for large-amplitude free vibration of shallow shells, it leads to the case that the linear in-plane modes are also dropped out from the analysis. The nonlinear Duffing modal equations are thus expressed in terms of linear bending modal amplitudes only. For shallow-shell structures, however, the bending component and in-plane component of each linear mode are inherently physically coupled as a result of curvature. By keeping in-plane inertia in the analysis and formulating the general Duffing equations in terms of the linearly coupled bending in-plane modal amplitudes, this yields a nonlinear response with the fixed ratio between the out-of-plane and in-plane deformation for each of the linear modes. This ratio, however, could be different at various large amplitudes for the nonlinear case. This is one of the objectives of the present paper to investigate the accuracy in predicting nonlinear frequency of shallow shells by the two distinct FE modal approaches. One uses the linearly coupled bending-in-plane modes without neglecting in-plane inertia, and the other employs the linear bending modes only and neglects the in-plane inertia.

The system equations of motion are formulated first in the physical structural node degrees of freedom (DOF). Then, the system is transformed into general Duffing-type modal equations with modal amplitudes in either coupled linear bending-in-plane modes or linear bending modes only. Linear bending-in-plane coupling is caused by the shell curvature as well as the nonsymmetric lamination ($[B] \neq 0$). Multiple modes and the first-order transverse shear deformation for composites are considered in the formulation. A triangular shallow-shell finite element is developed from an extension of the triangular Mindlin (MIN3) element with the improved shear correction factor by Tessler and Hughes[21] and Tessler.[22,23] Time-domain numerical integration is employed to determine nonlinear frequency of vibration with judicious initial conditions. Results obtained from two FE modal formulations are compared with classical and FE structural node DOF solutions, and conclusions are drawn regarding the accuracy of the proposed two FE modal formulations.

Formulation

Equations of Motion in Structure Node DOF

The in-plane strain, change of curvature, and shear-strain vectors based on the von Kármán large deflection and the first-order shear deformation theory for a doubly curved shallow shell presented in Fig. 1 are given by[10]

$$\{\varepsilon^0\} = \left\{\varepsilon_m^0\right\} + \left\{\varepsilon_b^0\right\} + \left\{\varepsilon_R^0\right\} = \begin{Bmatrix} u_{,x} \\ v_{,y} \\ u_{,y} + v_{,x} \end{Bmatrix} + \frac{1}{2}\begin{Bmatrix} w_{,x}^2 \\ w_{,y}^2 \\ 2w_{,x}w_{,y} \end{Bmatrix} + \begin{Bmatrix} w/R_x \\ w/R_y \\ 0 \end{Bmatrix}$$

$$\{\kappa\} = \begin{Bmatrix} \psi_{y,x} \\ \psi_{x,y} \\ \psi_{x,x} + \psi_{y,y} \end{Bmatrix}, \qquad \{\gamma_s\} = \begin{Bmatrix} w_{,y} \\ w_{,x} \end{Bmatrix} + \begin{Bmatrix} \psi_x \\ \psi_y \end{Bmatrix} - \begin{Bmatrix} u/R_x \\ v/R_y \end{Bmatrix} \quad (1)$$

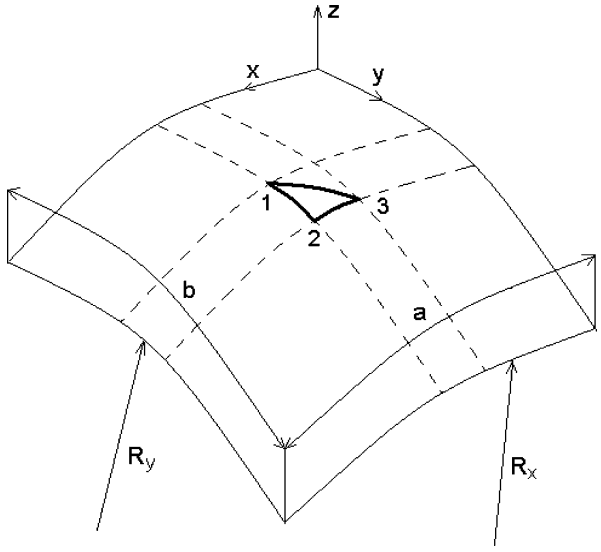

Fig. 1 Triangular shallow-shell finite element.

The constitutive equations for a laminated composite shallow-shell panel are[24]

$$\begin{Bmatrix} N \\ M \\ Q \end{Bmatrix} = \begin{bmatrix} A & B & 0 \\ B & D & 0 \\ 0 & 0 & A_s \end{bmatrix} \begin{Bmatrix} \varepsilon^0 \\ \kappa \\ \gamma_s \end{Bmatrix} \quad (2)$$

Applying the Hamilton's principle and standard finite element assembly procedure, the system equations of motion for a composite shallow shell undergoing large-amplitude free vibration can be expressed as[25]

$$\begin{bmatrix} M_b & 0 \\ 0 & M_m \end{bmatrix} \begin{Bmatrix} \ddot{W}_b \\ \ddot{W}_m \end{Bmatrix} + \left(\begin{bmatrix} K_b & K_{\mathrm{bm}} \\ K_{\mathrm{mb}} & K_m \end{bmatrix} + \begin{bmatrix} K_b^s & 0 \\ 0 & 0 \end{bmatrix} + \begin{bmatrix} K_b^R & K_{\mathrm{bm}}^R \\ K_{\mathrm{mb}}^R & 0 \end{bmatrix} + \begin{bmatrix} 0 & K_{\mathrm{bm}}^{sR} \\ K_{\mathrm{mb}}^{sR} & K_m^{sR} \end{bmatrix} + \begin{bmatrix} K1_b & K1_{\mathrm{bm}} \\ K1_{\mathrm{mb}} & 0 \end{bmatrix} + \begin{bmatrix} K1_b^{N_b} & 0 \\ 0 & 0 \end{bmatrix} + \begin{bmatrix} K1_b^{N_m} & 0 \\ 0 & 0 \end{bmatrix} + \begin{bmatrix} K1_b^{N_R} & 0 \\ 0 & 0 \end{bmatrix} + \begin{bmatrix} K1_b^R & 0 \\ 0 & 0 \end{bmatrix} + \begin{bmatrix} K2_b & 0 \\ 0 & 0 \end{bmatrix} \right) \begin{Bmatrix} W_b \\ W_m \end{Bmatrix} = \begin{Bmatrix} 0 \\ 0 \end{Bmatrix} \quad (3a)$$

or

$$[M]\{\ddot{W}\} + ([K_L] + [K1(W)] + [K2(W^2)])\{W\} = \{0\} \quad (3b)$$

The nonlinear stiffness matrices $[K1]$ and $[K2]$ depend linearly and quadratically on the unknown structural node DOF vector $\{W\}^T = \lfloor \{W_b\}^T, \{W_m\}^T \rfloor$, where $\{W_b\}^T = \lfloor \{W_t\}^T, \{\Psi_x\}^T, \{\Psi_y\}^T \rfloor$ and $\{W_m\}^T = \lfloor \{U\}^T, \{V\}^T \rfloor$. Solving the system of Eq. (3) turns out to be computationally costly because 1) at each time step the element nonlinear stiffness matrices are evaluated and the system nonlinear stiffness matrices are assembled and updated, 2) the number of structure node DOF of $\{W\}$ is usually very large, and 3) the time step of integration should be extremely small. An efficient solution procedure is to transform Eq. (3) into the modal coordinates[18–20,25] with a modal reduction. This is presented as follows.

Modal Formulation in Coupled Bending-In-Plane Modes

Express the panel deflection as a linear combination of some known functions as

$$\{W\} = \sum_{r=1}^{n} q_r(t)\{\phi\}^{(r)} = [\phi]\{q\} \quad (4)$$

where the number of retained linear modes is much smaller then the number of structure node DOF. The rth normal mode $\{\phi\}^{(r)T} = \lfloor \{\phi_b\}^{(r)T}, \{\phi_m\}^{(r)T} \rfloor$, which is the coupled bending-in-plane mode normalized with the maximum component to unity, and the linear natural frequency ω_r are obtained from the solution of the linear vibration problem

$$\omega_r^2[M]\{\phi\}^{(r)} = [K_L]\{\phi\}^{(r)} \tag{5}$$

where $[K_L] = [K] + [K^s] + [K^R] + [K^{sR}]$. Note that the relation between $\{\phi_b\}^{(r)}$ and $\{\phi_m\}^{(r)}$ is fixed. The modal mass matrix is

$$[\bar{M}] = [\phi]^T[M][\phi] \tag{6}$$

and the modal linear stiffness matrix is

$$[\bar{K}] = [\phi]^T[K_L][\phi] \tag{7}$$

Nonlinear stiffness matrices in modal coordinates[18,20,25] are defined as

$$[K_q] = [\phi]^T \sum_{r=1}^{n} q_r [K1]^{(r)}[\phi] \tag{8}$$

$$[K_{qq}] = [\phi]^T \sum_{r=1}^{n}\sum_{s=1}^{n} q_r q_s [K2]^{(rs)}[\phi] \tag{9}$$

Now, the equation of motion in the reduced amplitudes of coupled bending-in-plane modes has a form

$$\{\ddot{q}\} + [\bar{M}]^{-1}([\bar{K}] + [K_q] + [K_{qq}])\{q\} = \{0\} \tag{10}$$

Modal Formulation in Bending Modes Only

To express the shallow-shell response in terms of linear bending modes only, the in-plane inertia term in Eq. (3) must be neglected:

$$[M_m]\{\ddot{W}_m\} \cong \{0\} \tag{11}$$

This allows for the part of Eq. (3) corresponding to in-plane motion to be solved for in-plane displacement $\{W_m\}$ in terms of transverse displacement $\{W_b\}$ as

$$\{W_m\} = -\Big([K_m] + \left[K_m^{sR}\right]\Big)^{-1}\Big([K_{\mathrm{mb}}] + \left[K_{\mathrm{mb}}^{R}\right] + \left[K_{\mathrm{mb}}^{sR}\right] + [K1_{\mathrm{mb}}]\Big)\{W_b\} \tag{12}$$

whereas the part of Eq. (3) corresponding to the transverse and rotational motion becomes

$$[M_b]\{\ddot{W}_b\} + \Big([K_b] + \left\lfloor K_b^s \right\rfloor + \left\lfloor K_b^R \right\rfloor + [K1_b] + \left\lfloor K1_b^{N_b} \right\rfloor + \left\lfloor K1_b^{N_m} \right\rfloor + \left\lfloor K1_b^{R} \right\rfloor + \left\lfloor K1_b^{N_R} \right\rfloor + [K2_b]\Big)\{W_b\} + \underline{\Big([K_{\mathrm{bm}}] + \left[K_{\mathrm{bm}}^{R}\right] + \left[K_{\mathrm{bm}}^{sR}\right] + [K1_{\mathrm{bm}}]\Big)}\{W_m\} = \{0\} \tag{13}$$

Substitution of Eq. (12) into Eq. (13) results in the formulation when the in-plane inertia is neglected. It is observed that the cross product of the underlined portion of Eq. (13) by Eq. (12) will result in 16 new terms. It is further observed that among these 16 terms nine are linear and seven nonlinear. Then, the modal solution is sought in a form expressed in transverse and rotational degrees of freedom only, as

$$\{W_b\} = \sum_{r=1}^{n} q_r(t)\{\phi_b\}^{(r)} = [\phi_b]\{q\} \tag{14}$$

where $\{\phi_b\}^{(r)}$ are obtained from linear eigenproblem of a form

$$\omega_r^2[M_b]\{\phi_b\}^{(r)} = [K_{\mathrm{Lb}}]\{\phi_b\}^{(r)} \tag{15}$$

and $[K_{\mathrm{Lb}}]$ consists now of 12 linear terms listed in the Appendix [Eq. (A5)]. In particular, it is seen that this approach generates two additional second-order nonlinear terms being products of first-order nonlinear terms. The first of the two second-order nonlinear terms is generated by simple multiplication of two first-order nonlinear terms, and it becomes $-[K1_{\mathrm{bm}}]([K_m] + [K_m^{sR}])^{-1}[K1_{\mathrm{mb}}]$. The second of the two second-order nonlinear terms originates from the first-order nonlinear matrix $\lfloor K1_b^{N_m} \rfloor$. Because this term is expressed in function of $\{W_m\}$ [see Eq. (12)], two first-order nonlinearities are crossed resulting in a second-order nonlinear term of $\lfloor K2_b^{N_m} \rfloor$. As a result, the total second-order nonlinear stiffness when the in-plane inertia is neglected becomes as

$$[K2_b] - \underline{[K1_{\mathrm{bm}}]\Big([K_m] + \left[K_m^{sR}\right]\Big)^{-1}[K1_{\mathrm{mb}}] - \left[K2_b^{N_m}\right]} \tag{16}$$

where the underlined portion constitutes the difference in second-order nonlinear stiffness between the two modal formulations. Certainly, expressions for linear and first-order nonlinear terms are also differ as a result of assumption Eq. (11), but numerical results showed that this difference is minor (not greater than 2%), whereas differences in the second-order nonlinear term of Eq. (16) are substantial. Second-order nonlinear stiffness of the formulation involving assumption of Eq. (11) is always smaller; what would presumably result in more pronounced softening characteristics of the shallow-shell response. Detailed formulation in bending modes only is presented in the Appendix. The iterative procedure to determine the initial conditions providing the periodic solution was presented by Przekop et al.[20]

Results and Discussion

For all cases studied in this paper, only symmetrical shallow shells with respect to the two centerlines are considered. Subsequently the response consists only of symmetrical modes. This allows for a quarter of the shallow shell being studied for refined discretization. A 14×14 mesh size or 392 triangular shallow shell elements are used in FE discretizing model. The number of structural node DOF is 980.

Validation of the Formulation

The validation of the developed modal FE approach shown in Eq. (A6) was conducted by comparing the results obtained with classical formulation, which neglected the in-plane inertia and characterized the nonlinear vibration behavior with linear bending modes only. First, the FE single-mode solutions for isotropic shells supported by shear diaphragms were compared with analytical results obtained by Kobayashi and Leissa.[10] Figures 2–4 present the comparison of frequency ratios $\omega_{\mathrm{NL}}/\omega_L$ in function of nondimensional maximum deflection $W_{\max}/h$ for various shallow-shell geometries. Second, the coefficients of nonlinear terms of single-mode Duffing equation for a flat cross-ply plate were compared with Pillai and

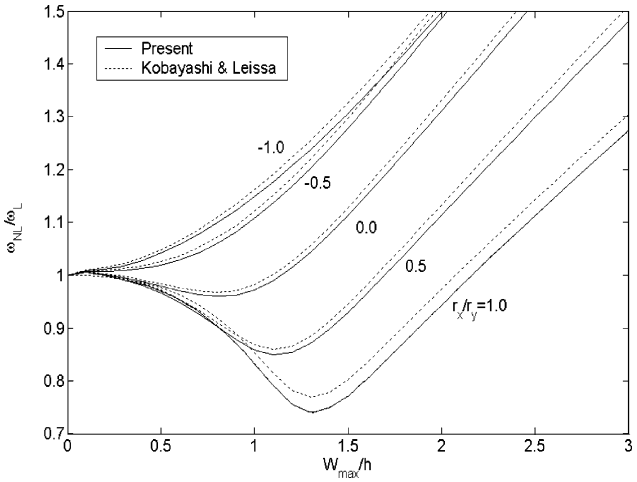

Fig. 2 Comparison of analytical and FE frequency ratio for various curvature ratios: $r_x = 10$, $h/a = 0.01$, $b/a = 1$, and $\nu = 0.3$.

Table 1 Duffing equation coefficients for a flat simply supported cross-ply $(0/90)_3$ rectangular plate, where $a = 20$ mm, $b = 10$ mm, $h = 0.6$ mm, $E_{11} = 5000$ kg/mm^2, $E_{22} = 500$ kg/mm^2, $\nu_{12} = 0.25$, and $G_{12} = 250$ kg/mm^2

$\ddot{q} + \omega^2(q + \alpha q^2 + \beta q^3) = 0$	α	β
PDE/Galerkin[14]	0.8896	5.9153
FE 14×14 mesh in quarter plate	0.8759	5.8965
Difference, %	−1.54	−0.32

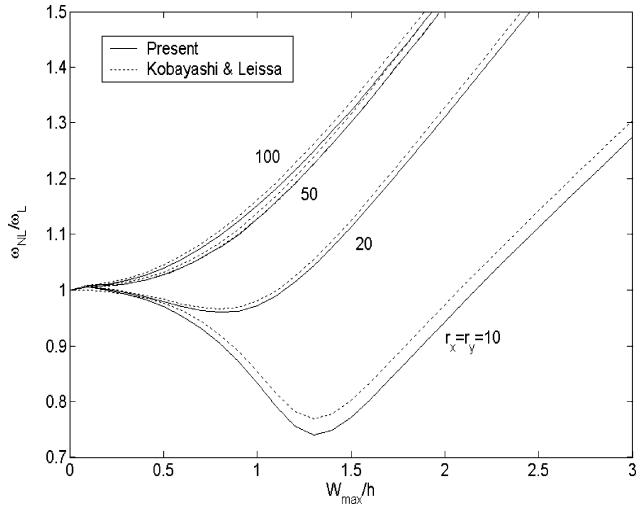

Fig. 3 Comparison of analytical and FE frequency ratio for various curvatures: $h/a = 0.001$, $b/a = 1$, and $\nu = 0.3$.

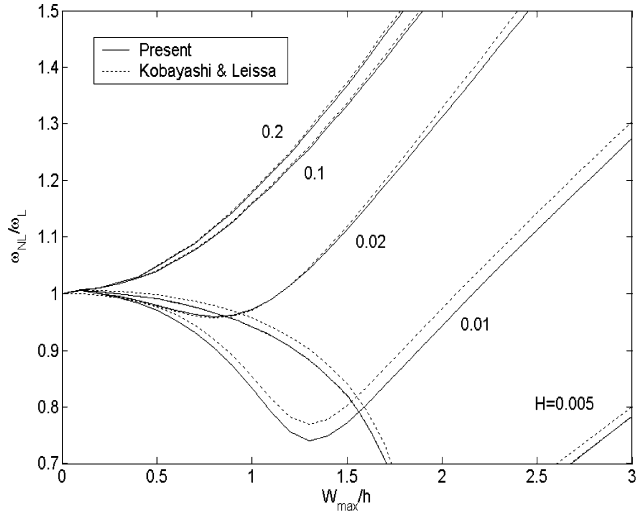

Fig. 4 Comparison of analytical and FE frequency ratio for various thickness ratios: $r_x = r_y = 10$, $b/a = 1$, $\nu = 0.3$, and $H = h/a$.

Rao[14] in Table 1. Therefore both factors, the curvature of the panel (Figs. 2–4) and the nonsymmetrical lamination sequence (Table 1), contributing to the quadratic and cubic terms in the Duffing equation are verified.

Subsequently, one of the square isotropic doubly curved shells with $r_x = r_y = 10$, $b/a = 1$, $H = 0.01$, and $\nu = 0.3$ (see Fig. 2), where $r_x = R_x/a$, $r_y = R_y/a$, and $H = h/a$, is studied further to investigate the difference in frequency ratios $\omega_{\mathrm{NL}}/\omega_L$ between the two sets of Duffing modal equations in terms of coupled bending-in-plane modes and bending modes only, and the discrepancy between single- and multimode solutions. Finally, several graphite-epoxy simply supported cylindrical panels are studied to determine the influence of varying lamination stacking on the response.

Table 2 Natural frequencies from Eq. (5) for isotropic square doubly curved shallow shell supported by shear diaphragms, where $a = b = 0.10$ m, $h = 1$ mm, and $R_x = R_y = 1$ m

Mode	Frequency, Hz
(1,1)	944.46
(1,3) + (3,1) or (1,3) − (3,1)	2550.6
(3,3)	4427.6

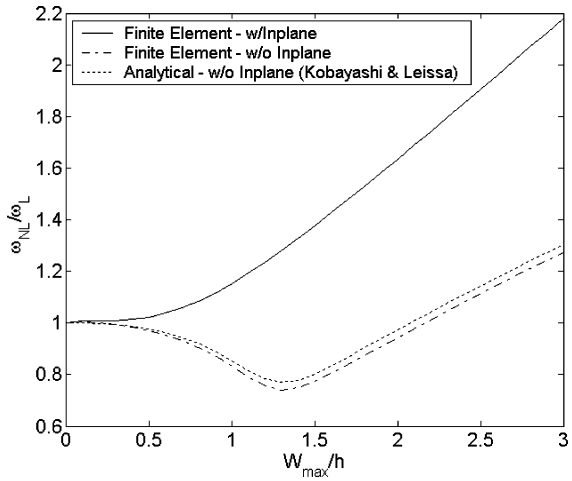

Fig. 5 Effect of in-plane inertia on the square isotropic doubly curved shallow-shell response: $\nu = 0.3$, $r_x = r_y = 10$, and $H = 0.01$.

Response Using Coupled Bending-In-Plane Modes vs Bending Modes Only

Analytical methods have expressed the shallow-shell response in terms of linear bending modes only by neglecting in-plane inertia as described earlier. The two FE formulations presented here are capable of providing solutions with and without this assumption. It is found, as presented in Fig. 5, that the vibrating shallow shell exhibits a hardening response characteristic when the solution is obtained by utilizing the coupled bending-in-plane modes with in-plane inertia included, and softening response characteristic when bending mode only is used and in-plane inertia effect is neglected. In attempt to resolve this ambiguity, three steps were undertaken, namely, 1) multimode solutions for both FE modal formulations were computed, 2) the solution in structural node DOF as presented in Eq. (3) was conducted, and 3) experimental verification of a clamped cylindrical shallow shell is currently underway, and the results will be presented in a follow-up paper.

Multimode Solution

The two-mode and three-mode solutions are determined and compared with single-mode solution using both FE modal formulations. Once the three-mode solution is available, also a solution in structural node DOF (caused by computational limitations a quarter of shallow shell was discretized with 8 by 8, or 128 triangular elements), with initial conditions obtained from the shell deflection of three-mode solution, is determined.

The first three natural frequencies from Eq. (5) are given in Table 2. Sample transverse and in-plane time responses and phase plot for moderately large-amplitude vibrations are presented in Figs. 6a, 6b, and 7, respectively, for the formulation in bending modes only. It is seen in Fig. 6 that the FE structural DOF solution (obtained with 8×8 mesh discretization) agreed very well with the three-mode modal solution using the Duffing equations in bending modes only (at $\omega/\omega_L = 0.9029$, $W_{\max}/h = 0.8899$, and $W_{\min}/h = -1.4858$). The transverse motion and the in-plane motion from the fundamental mode, three-mode, and structural node DOF solutions have the identical period of vibration or low frequency of $\omega/\omega_L = 0.9029$ shown in Figs. 6a and 6b, but not the same

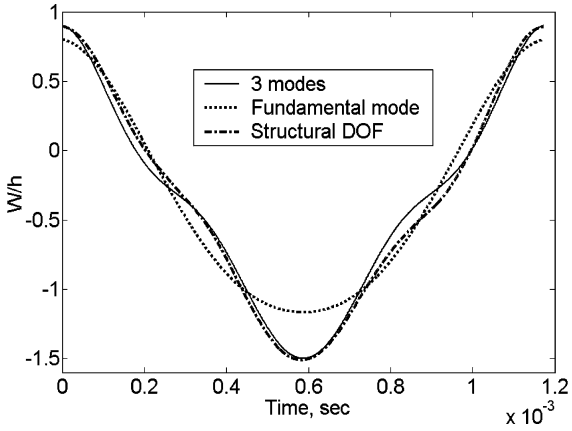

Fig. 6a Transverse time response of the center point of isotropic doubly curved shallow shell.

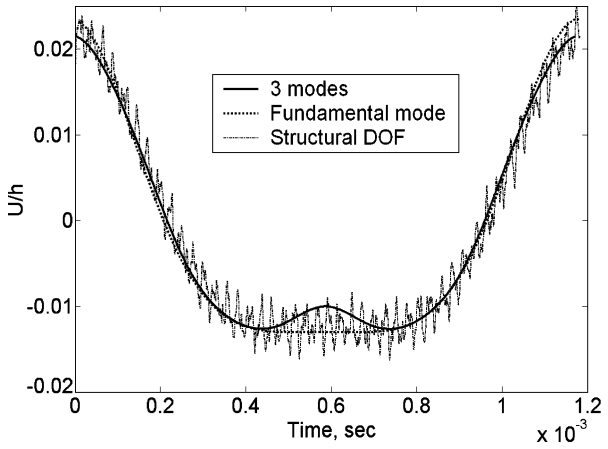

Fig. 6b In-plane time response of midedge point of isotropic doubly curved shallow shell.

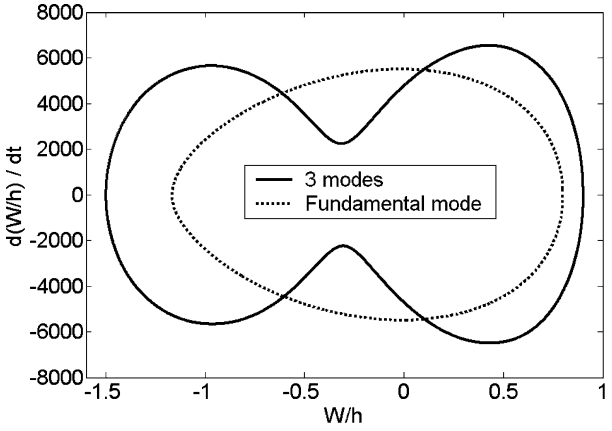

Fig. 7 Phase plot for isotropic doubly curved shallow shell.

$W_{\max}/h$ and $W_{\min}/h$. The extremely high frequency of the in-plane motion from the structural node DOF solution in Fig. 6b demonstrates clearly that the in-plane inertia can be neglected without loss of accuracy in prediction of nonlinear frequencies of vibration of shallow shells. For the same formulation, a typical set of the three-mode results consisting of the time response and the phase plots for each mode is presented in Figs. 8a and 8b, respectively. It is seen from the aforementioned figures that the multimode solution departs from the single-mode solution, especially for larger amplitudes in the inbound part of oscillation (compressive in-plane strain). For this reason, both values $W_{\max}/h$ and $W_{\min}/h$ are shown as a function of frequency ratio in Fig. 9, instead of $W_{\max}/h$ only, as it is traditionally done for isotropic or symmetrically laminated flat plates. The differences between the fundamental mode solution and multimode solutions are observed; however, the number of modes does not alter the solution characteristics between hardening and softening. On the other hand, it is seen that the substantial difference between the two modal FE formulations expressing the Duffing modal equations in terms of coupled bending-in-plane modes vs bending modes only. The formulation in terms of bending modes only is found to be accurate as verified by the results using structural node DOF shown in Figs. 6 and 9. It is apparent that the ratio between bending and in-plane displacements, which is constant for the linear case, does not hold constant because of the von Kármán type nonlinearity, and this ratio changes as the amplitude of vibration increases. Therefore expressing the nonlinear system response in terms of coupled linear bending and in-plane modes (with a fixed ratio between the bending and in-plane components of the eigenvector) acts as a constraint on the system, introducing an excessive amount of stiffening. This effect is demonstrated in Table 3 and Fig. 10. Based on the FE in structural DOF, and on the FE modal formulation that allows for adjustment between in-plane vs out-of-plane displacements, the ratio between maximum in-plane $U_{\max}/h = V_{\max}/h$ and transverse displacement $W_{\max}/h$ is calculated. It is seen that the ratio changes as the amplitude of the oscillation increases. Modal formulation in the linearly coupled bending-in-plane modes certainly would not allow for this adjustment, whereas the formulation in bending modes only

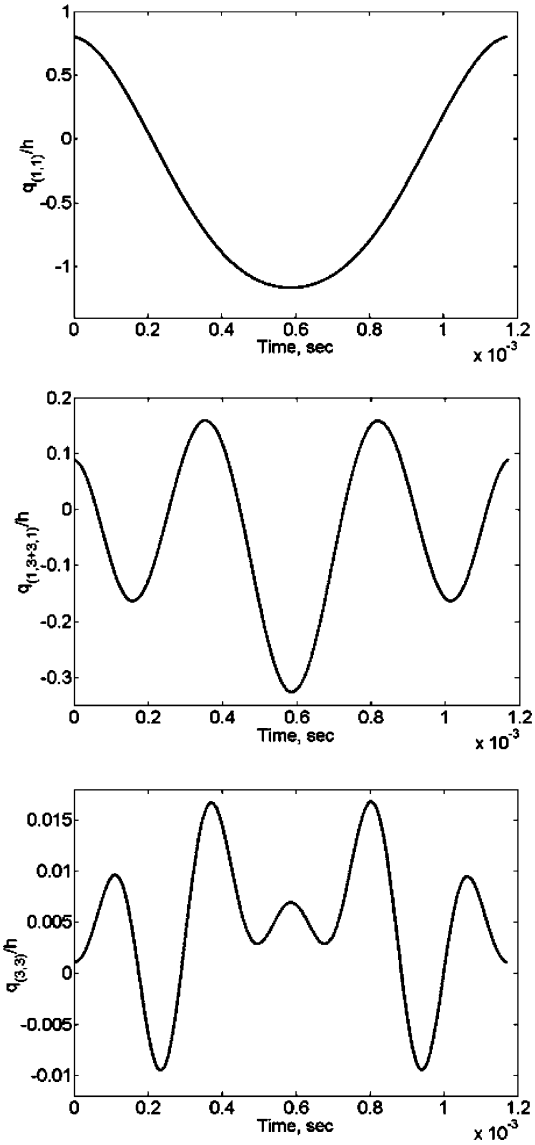

Fig. 8a Three-mode solution: time response for modes (1,1), (1,3) + (3,1), and (3,3).

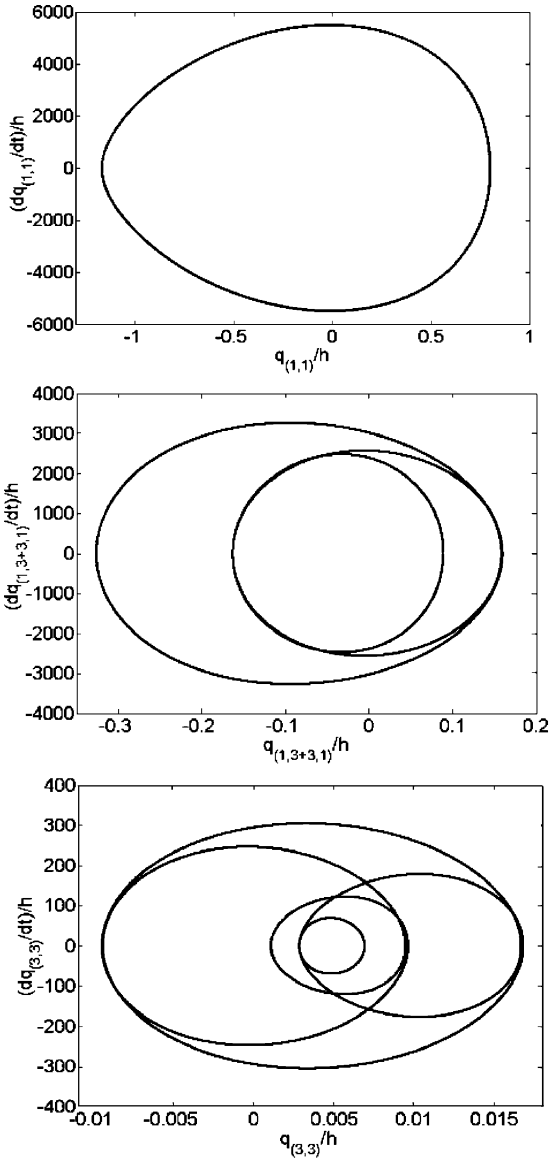

Fig. 8b Three-mode solution: phase plots for modes (1,1), (1,3) + (3,1), and (3,3).

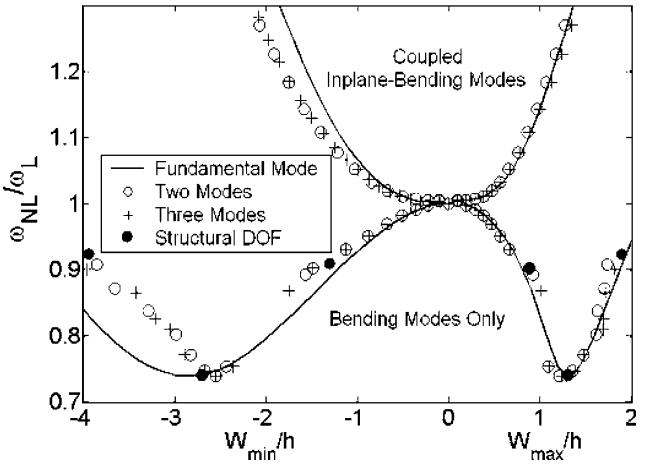

Fig. 9 Multiple-mode and single-mode solutions using the two distinct modal formulations vs structural node DOF solution for a isotropic doubly curved shallow shell.

Table 3 Ratios of in-plane vs out-of-plane displacement for various time instances during one period of oscillation for a doubly curved isotropic shell supported by shear diaphragms

	$(U_{max}/h)/(W_{max}/h) \times 100\%$	
W_{max}/h	Structural DOF	Three-mode solution
0.89	2.47	2.40
1.38	2.89	2.58
1.82	3.63	3.52

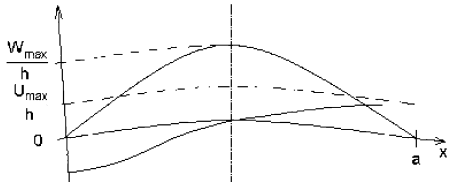

Fig. 10 Copuled linear bending in-plane $U_{max}/W_{max} = 2.07\%$.

does, as presented in Table 3 and Fig. 10. The differences observed between the ratios obtained via structural DOF and modal formulations are to be contributed to coarse discretization of structural DOF model and because of the low number of modes retained in the reduced-order solution.

Mode $(1,3)-(3,1)$ is not shown in Fig. 8 because it does not contribute to W_{max}/h and W_{min}/h. It is also seen in Fig. 9 that the FE solution in structural DOF compared very well with the FE modal solution in bending modes only. The value of contribution from the rth mode is defined as

$$\text{modal participation}(t) = \frac{|q_r(t)|}{\sum_{s=1}^{n} |q_s(t)|} \tag{17}$$

and in particular modal participation defined in Eq. (17) can be calculated at maximum deflection W_{max}, corresponding to time $t = kT$, and at minimum deflection W_{min}, corresponding to time $t = (k + \frac{1}{2})T$, where T is a period and $k = 0, 1, 2, \ldots$. Sample modal participation values for the case shown in Fig. 9 are given in Table 4, and it is seen that modal participations at W_{max} and W_{min} are not the same, and three modes will yield accurate converged frequency ratios.

Lamination Sequence

Responses of cylindrical rectangular simply supported graphite-epoxy composite panels with different lamination stacking, namely, antisymmetrical (0/90), (90/0), (0/90/0/90), and (90/0/90/0) and symmetrical (0/90/0) and (90/0/90) are investigated. Material properties are $E_1 = 26.24$ Msi (181.0 GPa), $E_2 = 1.49$ (10.3), $G_{12} = 1.04$ (7.17), $\nu_{12} = 0.28$, and $\rho = 0.1458 \times 10^{-3}$ lb-s^2/in.^{4} (1550 kg/m^3). For the (0/90) cylindrical panel, the (0) layer is closer to the center of cylinder. The composite shallow shell of the same planform dimensions 10×15 in. (0.254×0.381 m), curvatures $R_x = 100$ in. (2.54 m) and $R_y = \infty$, and thickness $h = 0.050$ in. (1.27 mm) is studied. A 14×14 mesh size or 392 triangular shallow shell elements are used to disretize a quarter of cylindrical panel. For simply supported boundary conditions the number of structural DOF is 980.

For antisymmetrical lamination stacking, additional linear bending-in-plane coupling occurs as a result of nonzero material stiffness $[B]$. This additional coupling can influence, depending of stacking sequence, the response characteristics, and either magnify or suppress softening effect. Although it was found in the preceding section that single-mode solution is not reasonably accurate, it was also found that additional modes added to the solution refine the results but will not alter softening vs hardening characteristics. Therefore the effect of laminate sequence study is performed using a single-mode solution. Because in the preceding section it was already concluded that modal FE formulation in terms of bending modes only yields accurate results, all of the composite shell cases are analyzed according to this formulation.

Table 4 Modal participations for isotropic doubly curved shallow shell

ω/ω_L	$w_{\max}/h$ $w_{\min}/h$	Modal participation at $W_{\max}$, % Modal participation at $W_{\min}$, % q_{11}	$q_{13}+q_{31}$	q_{33}
1.0044	0.0988	98.50	1.36	0.13
	−0.1055	98.41	1.47	0.12
0.9982	0.1950	97.03	2.70	0.28
	−0.2232	96.82	2.95	0.23
0.9917	0.2890	95.64	3.93	0.43
	−0.3553	95.15	4.52	0.33
0.9821	0.3813	94.42	4.99	0.59
	−0.5050	93.42	6.18	0.40
0.9695	0.4735	93.55	5.70	0.74
	−0.6768	91.52	8.04	0.45
0.9512	0.5685	93.32	5.79	0.89
	−0.8768	89.42	10.12	0.46
0.9307	0.6749	94.87	4.62	0.87
	−1.1227	86.63	12.85	0.51
0.9029	0.8899	89.90	9.98	0.12
	−1.4858	77.80	21.74	0.46
0.8692	1.0116	84.64	14.44	0.92
	−1.7477	87.06	11.93	1.01
0.7545	1.1022	89.87	8.73	1.40
	−2.3606	97.97	1.33	0.69
0.7396	1.2333	92.01	6.35	1.63
	−2.5480	96.16	3.20	0.65
0.7479	1.3773	95.57	2.99	1.44
	−2.6705	93.05	6.83	0.11
0.7717	1.4751	97.00	2.31	0.70
	−2.8952	91.07	8.29	0.65
0.8160	1.6895	88.54	4.13	7.33
	−3.0547	87.33	10.52	2.15
0.8260	1.6980	89.97	5.07	4.96
	−3.2144	88.71	10.40	0.89
0.8660	1.7116	90.14	6.85	3.02
	−3.4147	88.48	10.45	1.07
0.9010	1.8190	88.66	7.56	3.78
	−3.9575	88.94	10.17	0.89

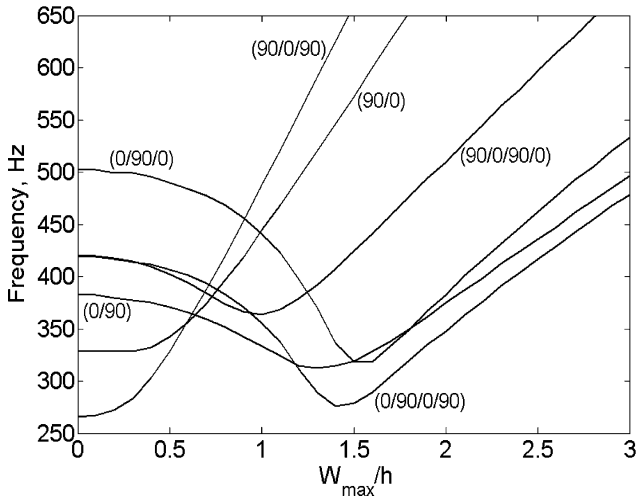

Fig. 11 Lamination stacking influence on the simply supported cylindrical rectangular panel response.

Table 5 presents the lowest three natural frequencies of the panels where the antisymmetrical lamination stacking is the strongest. As the sequence of lamination is reversed, the major differences are found with respect to natural frequencies, mode shapes, and nonlinear response characteristics. Lamination (0/90) results in the fundamental frequency being higher by 16.4% than for lamination (90/0). For (0/90) case, the sequence of mode shapes in increasing frequency is (1,1) followed by (3,1) and (1,3), whereas for (90/0) lamination sequence case the mode ordering is (1,1), (1,3), and (3,1). As for the nonlinear behavior, lamination sequence (0/90) introduces softening characteristics, whereas lamination (90/0) gives purely hardening response. More examples are illustrated in Fig. 11. Generally it is concluded that configurations with lower linear fundamental frequencies exhibit hardening response characteristics, whereas these of higher fundamental frequencies exhibit softening response characteristics.

Table 5 Natural frequencies for graphite-epoxy rectangular cylindrical simply supported panel with antisymmetrical lamination stacking

Lamination	Frequency, Hz Mode (1,1)	Mode (1,3)	Mode (3,1)
(0/90)	381.8	436.8	409.8
(90/0)	327.9	429.1	591.0

Conclusions

A major difference is found between the two modal finite element (FE) formulations: the one that expresses the Duffing equations in terms of coupled bending-in-plane modes and does not neglect in-plane inertia yields hard-spring behavior for the isotropic doubly curved shallow shell and the other that uses bending modes only and neglects in-plane inertia yields soft-spring behavior. Because analytical results are available only under the latter assumptions, FE solution in structural node DOF, which holds account of in-plane inertia and includes both out-of-plane and in-plane modes, is used to resolve the ambiguity. The formulation in terms of bending modes only is demonstrated to be accurate. This approach neglecting the in-plane inertia effects, however, does not result in an overstiffened solution because it allows adjustments for the bending vs in-plane strain, as the large amplitude of vibration changes. That property is an inherent feature of a formulation where von Kármań nonlinearity is involved. From the examples studied, it is concluded that two aforementioned modal FE formulations can give completely different characteristics (hard or soft spring), whereas multiple modes will improve the accuracy of the nonlinear frequency.

A vibrating flat plate always remains in tensile in-plane strain. For the shallow shell, the outbound part of oscillation is also associated with positive in-plane strain, but for the inbound part of oscillation the in-plane strain becomes negative. For that reason the time when shallow shell remains below the undeflected position is longer than half of the period, and the negative deflection has larger absolute value than positive deflection.

It is seen that even for moderate large deflection, the higher modes contribution could reach over 15% (Table 4). It is also observed that the modal participations differ based on the outbound (maximum) and inbound (minimum) deflections. The difference increases as the deflection increases.

Flexibility of enforcing complicated boundary conditions and nonrectangular geometries of the panel promote FE approach with the transformation into the modal degrees of freedom to be the essential tool for variety of shallow-shell panel response problems, including panel flutter, sonic fatigue, and postbuckling behavior.

Appendix: Finite Element Modal Formulation in Bending Modes Only

Substituting Eq. (12) into Eq. (13) yields

$$[M_b]\{\ddot{W}_b\} + \Big[[K_b] + \Big[K_b^s\Big] + \Big[K_b^R\Big] + [K1_b] + \Big[K1_b^{N_b}\Big] + \Big[K1_b^{N_m}\Big] + \Big[K1_b^R\Big] + \Big[K1_b^{C_R}\Big] + [K2_b] - \Big([K_{\rm bm}] + \Big[K_{\rm bm}^R\Big] + \Big[K_{\rm bm}^{sR}\Big] + [K1_{\rm bm}]\Big)\Big([K_m] + \Big[K_m^{sR}\Big]\Big)^{-1}\Big([K_{\rm mb}] + \Big[K_{\rm mb}^R\Big] + \Big[K_{\rm mb}^{sR}\Big] + [K1_{\rm mb}]\Big)\Big]\{W_b\} = \{0\} \quad \text{(A1)}$$

and it represents the equations of motion expressed in terms of bending displacement only. Expanding the bottom two lines of Eq. (A1),

16 new terms are generated. Nine of them are linear:

$$-[K_{\mathrm{bm}}]\left([K_m]+\left[K_m^{sR}\right]\right)^{-1}[K_{\mathrm{mb}}] \tag{A1a}$$

$$-[K_{\mathrm{bm}}]\left([K_m]+\left[K_m^{sR}\right]\right)^{-1}\left[K_{\mathrm{mb}}^{R}\right] \tag{A1b}$$

$$-[K_{\mathrm{bm}}]\left([K_m]+\left[K_m^{sR}\right]\right)^{-1}\left[K_{\mathrm{mb}}^{sR}\right] \tag{A1c}$$

$$-\left[K_{\mathrm{bm}}^{R}\right]\left([K_m]+\left[K_m^{sR}\right]\right)^{-1}[K_{\mathrm{mb}}] \tag{A1d}$$

$$-\left[K_{\mathrm{bm}}^{R}\right]\left([K_m]+\left[K_m^{sR}\right]\right)^{-1}\left[K_{\mathrm{mb}}^{R}\right] \tag{A1e}$$

$$-\left[K_{\mathrm{bm}}^{R}\right]\left([K_m]+\left[K_m^{sR}\right]\right)^{-1}\left[K_{\mathrm{mb}}^{sR}\right] \tag{A1f}$$

$$-\left[K_{\mathrm{bm}}^{sR}\right]\left([K_m]+\left[K_m^{sR}\right]\right)^{-1}[K_{\mathrm{mb}}] \tag{A1g}$$

$$-\left[K_{\mathrm{bm}}^{sR}\right]\left([K_m]+\left[K_m^{sR}\right]\right)^{-1}\left[K_{\mathrm{mb}}^{R}\right] \tag{A1h}$$

$$-\left[K_{\mathrm{bm}}^{sR}\right]\left([K_m]+\left[K_m^{sR}\right]\right)^{-1}\left[K_{\mathrm{mb}}^{R}\right] \tag{A1i}$$

six terms are first-order nonlinear:

$$-[K_{\mathrm{bm}}]\left([K_m]+\left[K_m^{sR}\right]\right)^{-1}[K1_{\mathrm{mb}}] \tag{A1j}$$

$$-\left[K_{\mathrm{bm}}^{R}\right]\left([K_m]+\left[K_m^{sR}\right]\right)^{-1}[K1_{\mathrm{mb}}] \tag{A1k}$$

$$-\left[K_{\mathrm{bm}}^{sR}\right]\left([K_m]+\left[K_m^{sR}\right]\right)^{-1}[K1_{\mathrm{mb}}] \tag{A1l}$$

$$-[K1_{\mathrm{bm}}]\left([K_m]+\left[K_m^{sR}\right]\right)^{-1}[K_{\mathrm{mb}}] \tag{A1m}$$

$$-[K1_{\mathrm{bm}}]\left([K_m]+\left[K_m^{sR}\right]\right)^{-1}\left[K_{\mathrm{mb}}^{R}\right] \tag{A1n}$$

$$-[K1_{\mathrm{bm}}]\left([K_m]+\left[K_m^{sR}\right]\right)^{-1}\left[K_{\mathrm{mb}}^{sR}\right] \tag{A1o}$$

and one term is second-order nonlinear:

$$-[K1_{\mathrm{bm}}]\left([K_m]+\left[K_m^{sR}\right]\right)^{-1}[K1_{\mathrm{mb}}] \tag{A1p}$$

Moreover, the matrix $\lfloor K1_b^{N_m}\rfloor$ depends on the in-plane displacement $\{W_m\}$; therefore, it will be also affected by the assumption of neglecting the in-plane inertia. Recalling the membrane displacement vector of Eq. (12),

$$\{W_m\}=-\left([K_m]+\left[K_m^{sR}\right]\right)^{-1}\left([K_{\mathrm{mb}}]+\left[K_{\mathrm{mb}}^{R}\right]+\left[K_{\mathrm{mb}}^{sR}\right]+[K1_{\mathrm{mb}}]\right)$$

$$\{W_b\}=-\left([K_m]+\left[K_m^{sR}\right]\right)^{-1}\left(\sum_{r=1}^{n}q_r(t)[K_{\mathrm{mb}}]\{\phi_b\}^{(r)}\right.$$
$$+\sum_{r=1}^{n}q_r(t)\left[K_{\mathrm{mb}}^{R}\right]\{\phi_b\}^{(r)}+\sum_{r=1}^{n}q_r(t)\left[K_{\mathrm{mb}}^{sR}\right]\{\phi_b\}^{(r)}$$
$$\left.+\sum_{r=1}^{n}\sum_{s=1}^{n}q_r(t)q_s(t)[K1_{\mathrm{mb}}]^{(r)}\{\phi_b\}^{(s)}\right) \tag{A2}$$

Therefore, the membrane vector, Eq. (A2), can be expressed in a form of

$$\{W_m\}=-\left(\sum_{r=1}^{n}q_r(t)\{W_m\}^{(r)}+\sum_{r=1}^{n}q_r(t)\left\{W_m^{R}\right\}^{(r)}\right.$$
$$\left.+\sum_{r=1}^{n}q_r(t)\left\{W_m^{sR}\right\}^{(r)}+\sum_{r=1}^{n}\sum_{s=1}^{n}q_r(t)q_s(t)\{W_m\}^{(rs)}\right) \tag{A3}$$

and then four new nonlinear modal matrices are generated from $\lfloor K1_b^{N_m}\rfloor$ matrix as following summation shows:

$$\left[K1_b^{N_m}\right]=-\sum_{r=1}^{n}q_r(t)[K1^{N_m}]^{(r)}-\sum_{r=1}^{n}q_r(t)[K1^{N_mR}]^{(r)}$$
$$-\sum_{r=1}^{n}q_r(t)[K1^{N_msR}]^{(r)}-\sum_{r=1}^{n}\sum_{s=1}^{n}q_r(t)q_s(t)[K2^{N_m}]^{(rs)} \tag{A4}$$

In particular, it is observed that this operation will yield a second-order nonlinear matrix, $\lfloor K2^{N_m}\rfloor$, and the final equation becomes

$$[M_b]\{\ddot{W}_b\}+[[K_b]+\left[K_b^{s}\right]+\left[K_b^{R}\right]-[K_{\mathrm{bm}}]\left([K_m]+\left[K_m^{sR}\right]\right)^{-1}[K_{\mathrm{mb}}]$$
$$-[K_{\mathrm{bm}}]\left([K_m]+\left[K_m^{sR}\right]\right)^{-1}\left[K_{\mathrm{mb}}^{R}\right]-[K_{\mathrm{bm}}]$$
$$\times\left([K_m]+\left[K_m^{sR}\right]\right)^{-1}\left[K_{\mathrm{mb}}^{sR}\right]-\left[K_{\mathrm{bm}}^{R}\right]\left([K_m]+\left[K_m^{sR}\right]\right)^{-1}$$
$$\times[K_{\mathrm{mb}}]-\left[K_{\mathrm{bm}}^{R}\right]\left([K_m]+\left[K_m^{sR}\right]\right)^{-1}\left[K_{\mathrm{mb}}^{R}\right]-\left[K_{\mathrm{bm}}^{R}\right]$$
$$\times\left([K_m]+\left[K_m^{sR}\right]\right)^{-1}\left[K_{\mathrm{mb}}^{sR}\right]-\left[K_{\mathrm{bm}}^{sR}\right]\left([K_m]+\left[K_m^{sR}\right]\right)^{-1}$$
$$\times[K_{\mathrm{mb}}]-\left[K_{\mathrm{bm}}^{sR}\right]\left([K_m]+\left[K_m^{sR}\right]\right)^{-1}\left[K_{\mathrm{mb}}^{R}\right]-\left[K_{\mathrm{bm}}^{sR}\right]$$
$$\times\left([K_m]+\left[K_m^{sR}\right]\right)^{-1}\left[K_{\mathrm{mb}}^{sR}\right]+[K1_b]+\left[K1_b^{N_b}\right]-\left[K1_b^{N_m}\right]$$
$$-\left[K1_b^{N_mR}\right]-\left[K1_b^{N_msR}\right]+\left[K1_b^{R}\right]+\left[K1_b^{N_R}\right]-[K_{\mathrm{bm}}]$$
$$\times\left([K_m]+\left[K_m^{sR}\right]\right)^{-1}[K1_{\mathrm{mb}}]-\left[K_{\mathrm{bm}}^{R}\right]\left([K_m]+\left[K_m^{sR}\right]\right)^{-1}$$
$$\times[K1_{\mathrm{mb}}]-\left[K_{\mathrm{bm}}^{sR}\right]\left([K_m]+\left[K_m^{sR}\right]\right)^{-1}[K1_{\mathrm{mb}}]-[K1_{\mathrm{bm}}]$$
$$\times\left([K_m]+\left[K_m^{sR}\right]\right)^{-1}[K_{\mathrm{mb}}]-[K1_{\mathrm{bm}}]\left([K_m]+\left[K_m^{sR}\right]\right)^{-1}$$
$$\times\left[K_{\mathrm{mb}}^{R}\right]-\left[K_{\mathrm{bm}}^{1}\right]\left([K_m]+\left[K_m^{sR}\right]\right)^{-1}\left[K_{\mathrm{mb}}^{sR}\right]+[K2_b]$$
$$-[K1_{\mathrm{bm}}]\left([K_m]+\left[K_m^{sR}\right]\right)^{-1}[K1_{\mathrm{mb}}]-[K2^{N_m}])\{W_b\}=\{0\} \tag{A5}$$

The modal equation in terms of bending modes only becomes

$$\lfloor\bar{M}_b\rfloor\{\ddot{W}_b\}+(\lfloor\bar{K}_{Lb}\rfloor+\lfloor\bar{K}_{qb}\rfloor+\lfloor\bar{K}_{qqb}\rfloor)\{W_b\}=\{0\} \tag{A6}$$

The modal transformation and the solution procedure follow exactly the one where the in-plane inertia is not neglected, with

$$\lfloor\bar{M}_b\rfloor=[\phi_b]^T[M_b][\phi_b] \tag{A6a}$$

$$\lfloor\bar{K}_b\rfloor=[\phi_b]^T[K_{Lb}][\phi_b] \tag{A6b}$$

$$[K_{qb}]=[\phi_b]^T\sum_{r=1}^{n}q_r(t)[K1_b(\phi)]^{(r)}[\phi_b] \tag{A6c}$$

$$\lfloor K_{qqb}\rfloor=[\phi_b]^T\sum_{r=1}^{n}\sum_{s=1}^{n}q_r(t)q_s(t)[K2_b(\phi)]^{(rs)}[\phi_b] \tag{A6d}$$

where $\lfloor K_{Lb}\rfloor$ is established in lines 2–6, $\lfloor K_{qb}\rfloor$ is established in lines 7–10, and $\lfloor K_{qqb}\rfloor$ is established in line 11 of Eq. (A5), respectively. For the detailed derivation, the readers are referred to Ref. 25.

Acknowledgments

L. Azrar acknowledges the assistance of a fellowship grant from the Fulbright Foundation and from the Maroccan–American Commission for Educational and Cultural Exchange during his stay at the Aerospace Engineering Department of Old Dominion University, Norfolk, Virginia.

References

[1]Leissa, A. W., "Vibration of Shells," NASA SP-288, April 1973.

[2]Kraus, H., *Thin Elastic Shells*, Wiley, New York, 1967, Chaps. 2 and 3.

[3]Libai, A., and Simmonds, J. G., *The Nonlinear Theory of Elastic Shells*, 2nd ed., Cambridge Univ. Press, Cambridge, England, U.K., 1998, Chaps. 7 and 8.

[4]Liew, K. M., Lim, C. W., and Kitipornchai, S., "Vibration of Shallow Shells: A Review with Bibliography," *Applied Mechanics Review*, Vol. 50, No. 8, 1997, pp. 431–444.

[5]Cummings, E. A., "Large Amplitude Vibration and Response of Curved Panels," *AIAA Journal*, Vol. 2, No. 4, 1964, pp. 709–716.

[6]Leissa, A. W., and Kadi, A. S., "Curvature Effects on Shallow Shell Vibrations," *Journal of Sound and Vibration*, Vol. 16, No. 2, 1971, pp. 173–187.

[7]Hui, D., "Influence of Geometric Imperfections and In-Plane Constraints on Nonlinear Vibrations of Simply Supported Cylindrical Panels," *Journal of Applied Mechanics*, Vol. 51, No. 2, 1984, pp. 383–390.

[8]Fu, Y. M., and Chia, C. Y., "Multi-Mode Non-Linear Vibration and Postbuckling of Anti-Symmetric Imperfect Angle-Ply Cylindrical Thick Panels," *International Journal of Non-Linear Mechanics*, Vol. 24, No. 5, 1989, pp. 365–381.

[9]Raouf, R. A., and Palazotto, A. N., "On the Nonlinear Free Vibration of Curved Orthotropic Panels," *International Journal of Non-Linear Mechanics*, Vol. 29, No. 4, 1994, pp. 507–514.

[10]Kobayashi, Y., and Leissa, A. W., "Large Amplitude Free Vibration of Thick Shallow Shells Supported by Shear Diaphragms," *Journal of Non-Linear Mechanics*, Vol. 30, No. 1, 1995, pp. 57–66.

[11]Shin, D. K., "Large Amplitude Free Vibration Behavior of Doubly Curved Shallow Open Shells with Simply-Supported Edges," *Computers and Structures*, Vol. 62, No. 1, 1997, pp. 35–49.

[12]Abe, A., Kobayashi, Y., and Yamada, G., "Nonlinear Vibration Characteristics of Clamped Laminated Shallow Shells," *Journal of Sound and Vibration*, Vol. 234, No. 3, 2000, pp. 405–426.

[13]Tamura, H., and Matsuzaki, K., "Numerical Scheme and Program for the Solution and Stability Analysis of a Steady Periodic Vibration Problem," *Japanese Society of Mechanical Engineering International Journal*, Vol. 39, No. 3, 1996, pp. 456–463.

[14]Pillai, S. R. R., and Rao, B. N., "Reinvestigation of Nonlinear Vibrations of Simply Supported Rectangular Cross-Ply Plates," *Journal of Sound and Vibration*, Vol. 160, No. 1, 1993, pp. 1–6.

[15]Bhimaraddi, A., "Large Amplitude Vibrations of Imperfect Antisymmetric Angle-Ply Laminated Plates," *Journal of Sound and Vibration*, Vol. 162, No. 3, 1993, pp. 457–470.

[16]Singh, A. V., "Linear and Geometrically Nonlinear Vibrations of Fiber Reinforced Laminated Plates and Shallow Shells," *Computers and Structures*, Vol. 76, No. 1–3, 2000, pp. 277–285.

[17]Sansour, C., Wagner, W., Wriggers, P., and Sansour, J., "An Energy-Momentum Integration Scheme and Enhanced Strain Finite Elements for the Nonlinear Dynamics of Shells," *International Journal of Nonlinear Mechanics*," Vol. 37, No. 4–5, 2002, pp. 951–966.

[18]Shi, Y., Lee, R. Y. Y., and Mei, C., "Finite Element Method for Nonlinear Free Vibration of Composite Plates," *AIAA Journal*, Vol. 35, No. 1, 1995, pp. 159–166.

[19]Abdel-Motaglay, K., Chen, R., and Mei, C., "Nonlinear Flutter of Composite Panels Under Yawed Supersonic Flow Using Finite Elements," *AIAA Journal*, Vol. 37, No. 9, 1999, pp. 1025–1032.

[20]Przekop, A., Azzouz, M. S., Guo, X., Mei, C., and Azrar, L., "Multimode Large Amplitude Vibration of Shallow Shells Considering In-Plane Inertia," AIAA Paper 2003-1772, April 2003.

[21]Tessler, A., and Hughes, T., Jr., "A Three-Node Mindlin Plate Element with Improved Transverse Shear," *Computer Methods in Applied Mechanics and Engineering*, Vol. 50, No. 1, 1985, pp. 71–101.

[22]Tessler, A., "A Priori Identification of Shear Locking and Stiffening in Triangular Mindlin Elements," *Computer Methods in Applied Mechanics and Engineering*, Vol. 53, No. 2, 1985, pp. 183–200.

[23]Tessler, A., "A C°-Anisoparametric Three-Node Shallow Shell Element," *Computer Methods in Applied Mechanics and Engineering*, Vol. 78, No. 1, 1990, pp. 89–103.

[24]Reddy, J. N., *Mechanics of Laminated Composite Plates*, CRC Press, Boca Raton, FL, 1997, pp. 164, 165.

[25]Przekop, A., "Nonlinear Response and Fatigue Estimation of Aerospace Curved Surface Panels to Acoustic and Thermal Loads," Ph.D. Dissertation, Dept. of Aerospace Engineering, Old Dominion Univ., Norfolk, VA, Aug. 2003.

A. Berman
Associate Editor